

## Computer prediction of fracture of magnesium alloy cylindrical billet during equal channel angular pressing

*Elena P. Volkova*<sup>1</sup>, junior researcher

of the Research Institute of Physics of Advanced Materials

*Gandzhina D. Khudododova*<sup>2</sup>, junior researcher

of the Research Institute of Physics of Advanced Materials

*Aleksandr V. Botkin*<sup>3</sup>, Doctor of Sciences (Engineering),

professor of Chair of Materials Science and Physics of Metals

*Ruslan Z. Valiev*<sup>\*4</sup>, Doctor of Sciences (Physics and Mathematics), Professor,

Director of the Research Institute of Physics of Advanced Materials

*Ufa University of Science and Technology, Ufa (Russia)*

\*E-mail: ruslan.valiev@ugatu.su

<sup>1</sup>ORCID: <https://orcid.org/0009-0004-7183-4077>

<sup>2</sup>ORCID: <https://orcid.org/0000-0002-1273-8518>

<sup>3</sup>ORCID: <https://orcid.org/0000-0001-9522-280X>

<sup>4</sup>ORCID: <https://orcid.org/0000-0003-4340-4067>

Received 03.05.2024

Revised 18.09.2024

Accepted 21.10.2024

**Abstract:** The main challenge in using magnesium alloys, applied in medicine as biodegradable materials, is their difficult deformability, which in turn leads to frequent failure of samples during severe plastic deformation. This paper shows that the temperature mode of equal channel angular pressing (ECAP) of a Mg–Zn–Ca system magnesium alloy, which ensures deformation of samples without failure, can be determined based on the results of finite-element computer simulation of the stress-strain state of the billet, calculation of alloy damage using the Cockcroft–Latham model, and prediction of the sample failure area. Modelling showed that the surface area of the billet adjacent to the matrix inner corner during ECAP, is the area of possible failure of the magnesium alloy. The value of alloy damage during ECAP in this area at  $T=350$  °C is less than 1, which corresponds to non-failure of the metal. To verify the computer simulation results, ECAP physical simulation was performed; billets without signs of failure were produced. A study of the mechanical properties of the Mg–1%Zn–0.06%Ca magnesium alloy was conducted before and after ECAP processing according to the selected mode: the ultimate strength limit increased by 45 %, the hardness increased by 16 %, while the plasticity increased by 5 %.

**Keywords:** magnesium alloys; stress-strain state; finite-element computer simulation; alloy damage; equal channel angular pressing; microhardness; ultimate strength limit.

**Acknowledgments:** The work was supported by the Russian Science Foundation, project No. 24-43-20015 (<https://rscf.ru/project/24-43-20015/>). The experimental part was carried out using the equipment of the “Nanotech” Shared Research Facility of Ufa University of Science and Technology.

**For citation:** Volkova E.P., Khudododova G.D., Botkin A.V., Valiev R.Z. Computer prediction of fracture of magnesium alloy cylindrical billet during equal channel angular pressing. *Frontier Materials & Technologies*, 2024, no. 4, pp. 19–28. DOI: 10.18323/2782-4039-2024-4-70-2.

### INTRODUCTION

In the last decade, magnesium alloys have attracted increased attention from researchers studying biomaterials for medical use. These alloys contain chemical elements that interact beneficially with the human body. However, these alloys in the cast state have low strength, and corrosion resistance for their successful application when producing biosoluble implants used in maxillofacial surgery and orthopaedics [1; 2]. In this work, to increase the strength of the Mg–1%Zn–0.06%Ca alloy, one of the effective approaches was used – the formation of an ultrafine-grained structure in them by the severe plastic deformation methods [3–5], namely, processing of billets by equal channel angular pressing (ECAP).

Cast magnesium alloys are difficult-to-form materials, have low plasticity during deformation at room temperature, and are prone to destruction [6–8]. In experimental studies, the temperature of deformation treatment is often determined empirically, which requires considerable time and material resources. The use of models of metal destruction, during pressure treatment, is an alternative to the experimental determination of the temperature regime.

In the mechanics of pressure metal treatment, a quantitative assessment of damage [9] – microscopic discontinuities (submicro- and micropores, microcracks) of the metal is performed using indirect relative indicators. For example, according to the methodology of V.L. Kolmogorov,

A.A. Bogatov<sup>1</sup>, the metal damage in the material point of the deformed body, is the ratio of the strain degree accumulated by the material point during the deformation process, to the maximum possible degree of metal strain accumulated by the moment of exhaustion of the ability to deform without fracture, i.e. by the moment of accumulation of the metal maximum damage equal to 1, when macrocracks occur in an avalanche-like manner – this moment is called destruction. If the accumulation of maximum damage equal to 1 occurs at a material point on the surface of a deformed specimen, then the metal fracture at this point on the surface is visually detected by the appearance of a crack. If the accumulation of maximum damage equal to 1 occurs at any material point inside a deformed specimen, then the metal fracture at this point in the form of a pore is detected not visually, but using special equipment, for example, a device using ultrasonic radiation.

In [10], it was shown for the first time that metal damage within the Cockcroft–Latham model can be quantitatively and indirectly calculated, taking into account the changing stress state, as the ratio of the specific work of positive internal forces (principal normal positive stresses), acting on a material point during deformation to the maximum possible specific work of positive internal forces, corresponding to the moment when the metal exhausts its ability to deform without destruction. In [11; 12] it is shown that the normalised Cockcroft–Latham fracture model has a higher accuracy of predicting cracks in various technological processes. This approach was further developed in [13; 14].

As noted in [15], the difficulty of choosing and optimising the ECAP scheme is that the wall flow fields, "overhardening" and hidden damage are difficult to observe and poorly predicted. Therefore, the development of new and verification of existing methods for predicting metal fracture during ECAP, especially when applied to magnesium alloys, is an urgent and important task. A promising solution to this problem is the use of computer simulation to analyse the processes of billet damage during ECAP, which is based on predicting the area of sample fracture [16].

The purpose of this study is to determine, using computer simulation, such a temperature mode of equal channel angular pressing (ECAP) of Mg–Zn–Ca alloy, which ensures deformation of samples without fracture, and the achievement of increased mechanical properties in the alloy.

## METHODS

The conducted studies included a physical experiment and finite-element computer simulation of the stress-strain state of the billet in the DEFORM-3D software package, as well as calculation of alloy damage.

The initial cylindrical samples (billets) of Mg–1%Zn–0.06%Ca magnesium alloy with a diameter of 20 mm and a length of 100 mm for physical simulation were made on

a lathe from a round cast produced by gravity casting. The Mg–1%Zn–0.06%Ca alloy was cast at the Solikamsk Experimental Metallurgical Plant (Russia). The chemical composition was determined using a Thermo Fisher Scientific ARL 4460 OES optical emission spectrometer (USA), and is presented in Table 1. In order to equalise the chemical composition throughout the sample volume, and eliminate the effects of dendritic liquation, the cast samples were heat-treated (subjected to homogenization annealing) in a Nabertherm muffle furnace at 450 °C for 24 h with cooling in water [17]. This state of the sample was taken as the initial one.

Physical simulation was performed on an ECAP equipment manufactured with an intersection angle of cylindrical channels of 120°. The tooling was heated to the required temperature using two electric heating elements in the form of clamps installed on the matrix. Before ECAP, the initial billet was heated in a chamber resistance furnace to the required temperature. Each subsequent ECAP pass was performed with a 90° rotation around the longitudinal axis of the billet. ECAP processing was carried out according to the mode described in [18] for the Mg–Zn–Ca system alloy: the first and second passes were performed at 400 °C; the third and fourth – at 350 °C; the fifth and sixth – at 300 °C; the seventh and eighth – at 250 °C.

At the first stage of theoretical research, a thermoplastic problem was solved using the DEFORM-3D software product: the non-uniform stress-strain state in the volume of the billet was determined stepwise. Finite-element computer simulation of the billet stress-strain state during ECAP (Fig. 1) was carried out under the following assumptions (usually used in modelling practice):

- 1) the problem was solved under conditions of a volumetric stress-strain state;
- 2) under non-isothermal conditions, taking into account the thermal effect of plastic deformation at the initial temperature of the billet (20...350) °C;
- 3) the billet material model is a plastic medium, the yield stress dependences on the degree of deformation of the Mg–1%Zn–0.06%Ca alloy, obtained from the results of preliminary mechanical tensile tests in the temperature and strain rate ranges corresponding to those realised during ECAP, were entered in tabular form during the preparation of the database;
- 4) the matrix and punch material for ECAP is a non-deformable rigid medium with a temperature of (20...350) °C.

The punch movement speed was set constant at 0.56 mm/s (equal to the movement speed of the movable crosshead of the hydraulic press during ECAP, with a nominal force of 160 tf). The  $\psi$  index of friction (according to Siebel) between the tool and the billet was taken equal to 0.3, and determined based on the results of preliminary virtual and physical modelling of the longitudinal upsetting of samples using graphite-molybdenum lubricant. The simulation was performed using a uniform grid of elements. The minimum size of the finite element (the length of the tetrahedron edge) was 1.2 mm. Verification of the results of computer simulation with the specified assumptions, the number of finite elements and the results of physical modelling of

<sup>1</sup> *Plasticity and destruction / edited by V.L. Kolmogorov. M.: Metallurgy, 1977. 336 p.*

Table 1. Chemical composition of the Mg-1%Zn-0.06%Ca alloy  
Таблица 1. Химический состав сплава Mg-1%Zn-0,06%Ca

Element mass content										
Zn	Zr	Al	Fe	Mn	Ni	Cu	Si	Ca	Pb	Sn
0.953	≤0.001	0.011	0.027	0.0026	0.0008	0.0008	0.0025	0.0641	0.018	≤0.001

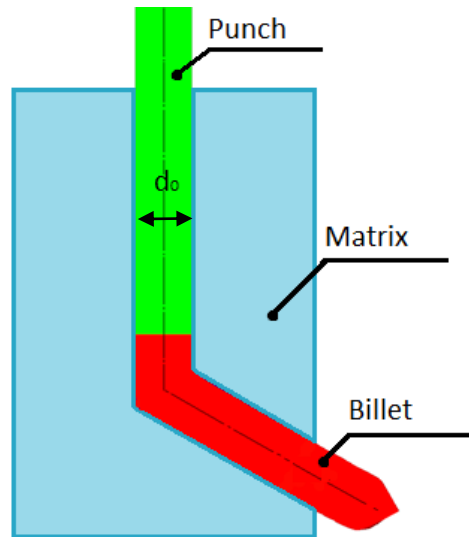


Fig. 1. ECAP equipment diagram  
Рис. 1. Схема оснастки для РКУП

ECAP, showed a relative excess of the calculated deformation force over the value experimentally measured at the quasi-stationary stage of ECAP by 5 %.

At the second stage, the alloy damage was calculated using the results of simulating the billet stress-strain state during ECAP, and the well-known Cockcroft–Latham fracture model [19].

In the DEFORM-3D software package for predicting the failure of metals and alloys under large plastic deformation, the Cockcroft–Latham fracture model is traditionally used as the main technique. However, it does not take into account the effect of the metal stress state on the maximum possible value of the specific work of positive internal forces, corresponding to the moment when the metal exhausts its ability to deform without failure.

According to the Cockcroft–Latham fracture model, the condition of nonfailure of a material point is verified by the inequality:

$$c < c_{ult}, \tag{1}$$

where the left-hand side of the inequality  $c = \int_0^{\varepsilon_i} \frac{\sigma_1}{\sigma_i} d\varepsilon_i$  is the damage index, the Cockcroft–Latham energy index of the relative specific work of elementary tensile forces,

$\sigma_1$  is the principal positive normal stress,

$\sigma_i$  is the stress intensity,

$\varepsilon_i$  is the deformation intensity;

$c_{ult}$  is the ultimate (maximum possible) value of the Cockcroft–Latham index corresponding to the moment of metal fracture.

Metal fracture in accordance with the Cockcroft–Latham fracture model occurs when the condition  $c \geq c_{ult}$  is met.

The damage was calculated using the formula obtained in [10] that takes into account the effect of the stress state on the ultimate (maximum possible) value of the Cockcroft–Latham index:

$$\omega = \sum_{k=1}^r \frac{\Delta C_k}{\left( \left( \frac{\sigma_1}{\sigma_i} \right)_{av} \varepsilon_{i,p} \right)_k}, \tag{2}$$

where  $r$  is the number of stages of deformation of the material point;

$\Delta C_k = \int_{\varepsilon_{i,k}}^{\varepsilon_{i,k+1}} \frac{\sigma_1}{\sigma_i} d\varepsilon_i$  is the increment of the Cockcroft–Latham index (the increment of the specific work of the positive internal forces acting on the material point at the  $k$ -th stage of deformation of the billet material point);

$\varepsilon_{i, k}$  is the degree of deformation accumulated by the material point of the billet by the beginning of the  $k$ -th stage of deformation;

$\varepsilon_{i, k+1}$  is the degree of deformation accumulated by the material point of the billet by the end of the  $k$ -th stage of deformation;

$\sigma_1$  is the principal positive normal stress;

$\sigma_i$  is the stress intensity;

$(\sigma_1/\sigma_i)_{av}$  is average value of the ratio of the principal normal stress to the stress intensity at the  $k$ -th stage of deformation of the material point of the billet;

$\varepsilon_{i,p}$  is degree of deformation accumulated by the material point of the sample by the moment of fracture (quantitative measure of alloy plasticity) at a constant value of the  $\sigma_1/\sigma_i$  stress state index.

Functions

$$\varepsilon_{i,p} = -0.19 \ln \left( \frac{\sigma_1}{\sigma_i} \right) + 0.16; \tag{3}$$

$$\varepsilon_{i,p} = -0.21 \ln \left( \frac{\sigma_1}{\sigma_i} \right) + 0.18,$$

determining the plasticity of the Mg–1%Zn–0.06%Ca magnesium alloy at temperatures of 20 and 350 °C, depending on the stress state index were found experimentally using the method given in [20].

To take into account the change in the stress state index of the material point, the damage in it was calculated for  $r=150$  stages, while the duration of all deformation stages was the same and equal to  $t_s=1$  s, satisfying the condition [10]:

$$0.99 \leq \frac{\sum_{k=1}^r \left[ \left( \frac{\sigma_1}{\sigma_i} \right)_{av} t_s \right]_k}{S} \leq 1, \tag{4}$$

where  $S$  is the area determined using the graph of the stress state index  $\sigma_1/\sigma_i$  of the material point of the billet, versus the deformation time. The alloy damage during ECAP was calculated for the material point, with the maximum value of the  $c$  damage index in the billet area determined, based on the simulation results.

The calculation of the alloy damage using formulas (2), (3), and the results of modelling the stress-strain state of the billet was performed in Excel, since the DEFORM-3D software product developers do not provide the ability for a user to enter any constitutive relations, metal fracture models, etc. into the solver.

Microhardness (HV) was measured using the Vickers method on an Emco-Test Durascan 50 micro-macrohardness tester, with an indenter load of 0.49 N and a holding time of 10 s. Microhardness measurements were performed using disk-shaped specimens with a diameter of 20 mm and a thickness of 1.5 mm, cut in the transverse direction from a deformed billet. For each specimen, 20 measurements were taken. Tensile tests were performed on an Instron 5982 testing machine at room temperature

and a strain rate of  $10^{-3} \text{ s}^{-1}$  on the specimens with a working part size of  $0.6 \times 1 \times 4.5 \text{ mm}^3$ . Flat specimens were cut from the disk-shaped samples. At least 5 specimens were tested for each condition.

## RESULTS

### Results of computer simulation

The distribution of the damage index obtained by computer simulation showed that the surface area of the billet, adjacent to the inner corner of the matrix during ECAP, is the area of possible fracture of the magnesium alloy (Fig. 2). The point from this area indicated in Fig. 2 enters the plastic deformation zone when the matrix outlet channel is completely filled with the alloy, i.e., at the steady-state stage of ECAP.

A significant increase in the  $c$  damage index (Fig. 3) at the point of the billet occurs in the time interval of 68–85 s due to the action of the  $\sigma_1$  positive normal stress (Fig. 4).

The degree of deformation (Fig. 5) at the material point in the time range of 68–85 s, as well as the damage index, increases.

The value of metal damage at  $T=20$  °C calculated by formula (2) was obtained equal to  $\omega=1.19$ . Therefore, the condition  $\omega < 1$  is not met, and the billet will fail during ECAP deformation in the first pass in the area of the surface adjacent during ECAP to the inner corner of the matrix. The calculated value of the alloy damage at  $T=350$  °C was obtained as  $\omega=0.9$ , which is less than 1, the nonfailure condition of the metal  $\omega < 1$  is met, and the billet will not fail during the first pass of ECAP.

### Physical experiment results

Fig. 6 a shows an image of sample 1 deformed in one pass at room temperature – the sample failed into two separate parts. One of the parts shows a macrocrack in the area of the billet adjacent during deformation to the inner corner of the matrix. Fig. 6 b shows an image of sample 2 deformed in one pass at  $T=400$  °C – there are no visible signs of failure on the sample. The results of the studies of the mechanical properties of the samples are shown in Fig. 7 and listed in Table 2.

Fig. 7 a shows the stress-strain diagram of the studied alloy before and after ECAP. The Mg–1%Zn–0.06%Ca alloy in the homogenised state has a strength of 144 MPa. In the deformed state, its strength increased with an increase in the strain degree using the ECAP method. Thus, after 8 ECAP passes, the strength increased to 210 MPa, which is 45 % higher compared to the alloy in the homogenised state (Fig. 7 a, Table 2). The yield strength increased significantly – from 42 MPa in the homogenised state to 68 MPa after ECAP deformation. This result indicates the importance of ECAP for increasing the strength properties of this alloy. The microhardness of the homogenised state of the Mg–1%Zn–0.06%Ca alloy was  $44 \pm 2.8$  HV. The microhardness value increased from  $44 \pm 2.8$  to  $51.2 \pm 3.4$  HV as a result of plastic deformation by the ECAP method, with a strain degree of  $\varepsilon=5.04$ , accumulated over 8 passes (Fig. 7 b, Table 2).

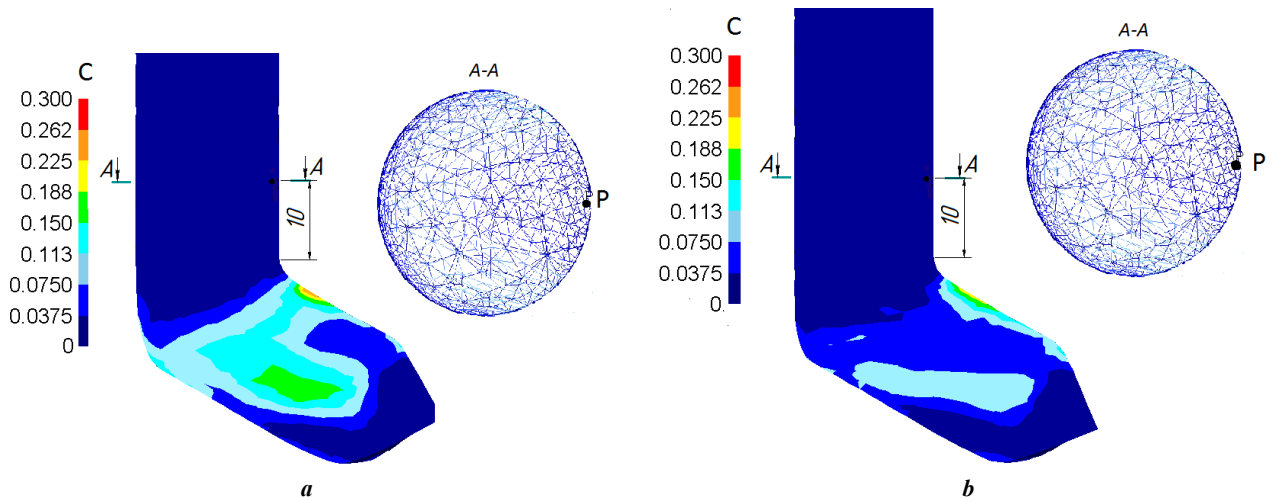


Fig. 2. Scheme of the position of the material point selected for damage calculation and the distribution of the  $c$  index in the longitudinal section of the virtually deformed billet at the initial temperature:

$a - T=20\text{ }^{\circ}\text{C}$ ;  $b - T=350\text{ }^{\circ}\text{C}$

Рис. 2. Схема положения материальной точки, выбранной для расчета поврежденности, и распределение показателя  $c$  в продольном сечении виртуально деформированной заготовки при начальной температуре:

$a - T=20\text{ }^{\circ}\text{C}$ ;  $b - T=350\text{ }^{\circ}\text{C}$

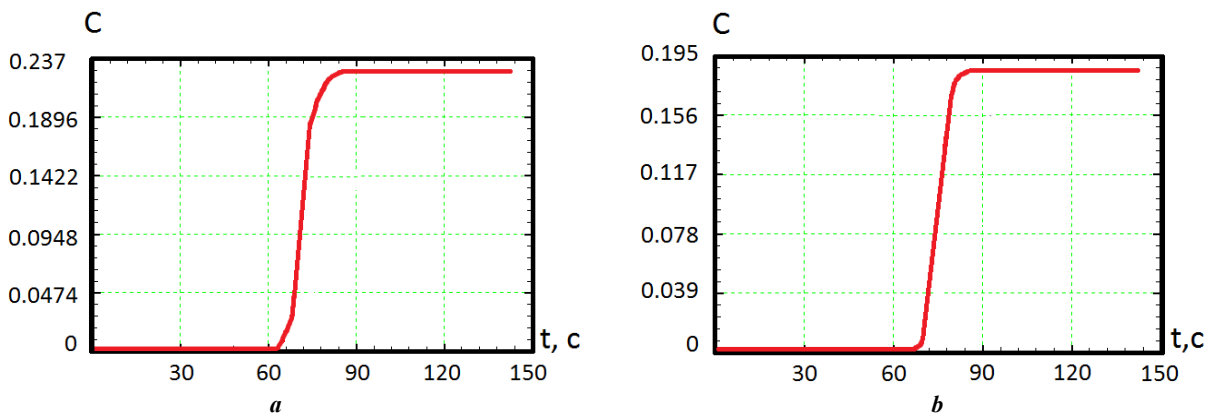


Fig. 3. Change in damage index over time at a point:  $a - T=20\text{ }^{\circ}\text{C}$ ;  $b - T=350\text{ }^{\circ}\text{C}$

Рис. 3. Изменение во времени показателя поврежденности в точке:  $a - T=20\text{ }^{\circ}\text{C}$ ;  $b - T=350\text{ }^{\circ}\text{C}$

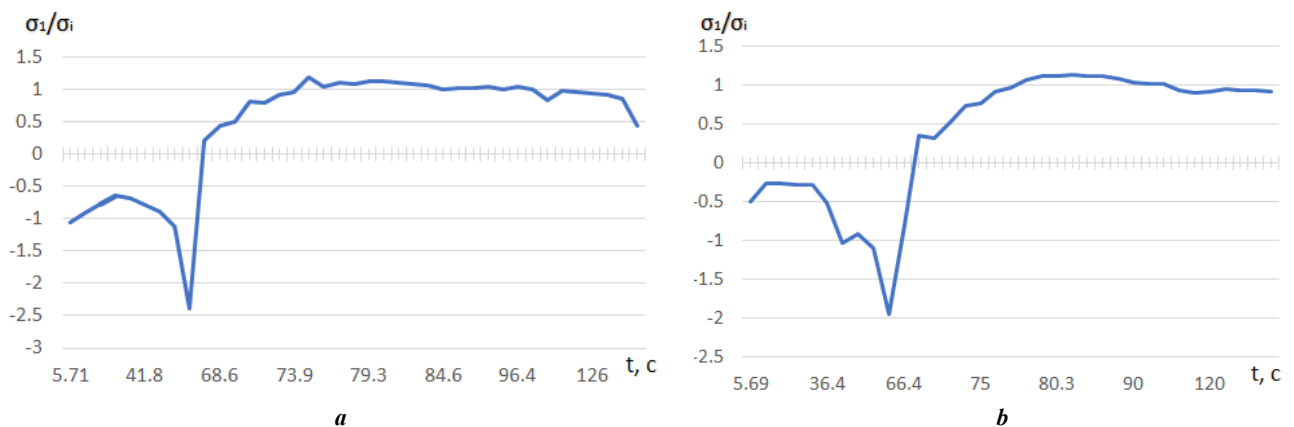
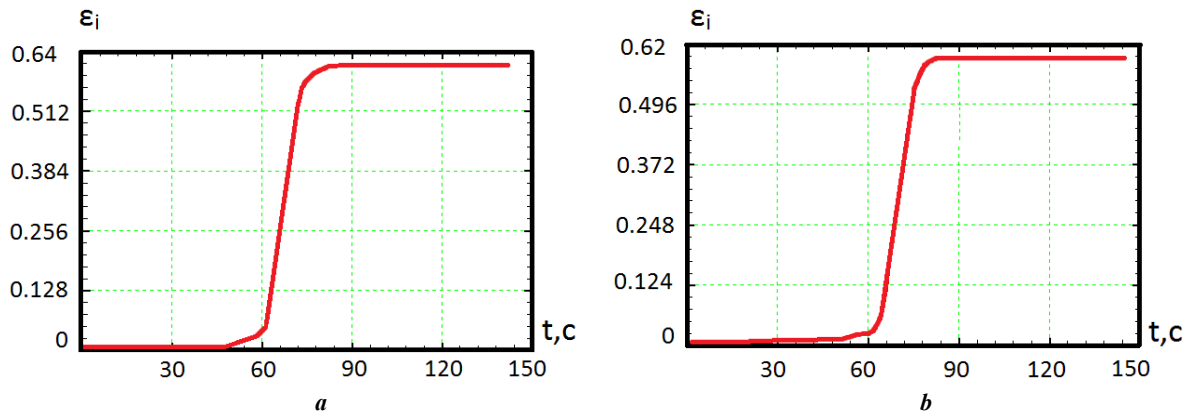


Fig. 4. Change of the  $\sigma_1/\sigma_i$  index of the stress state at a material point of the billet over time:

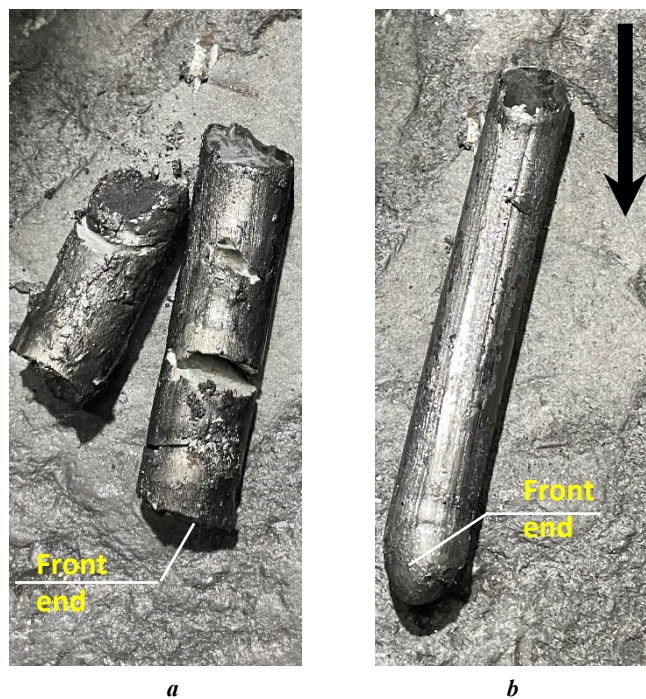
$a - T=20\text{ }^{\circ}\text{C}$ ;  $b - T=350\text{ }^{\circ}\text{C}$

Рис. 4. Изменение во времени показателя  $\sigma_1/\sigma_i$  напряженного состояния в материальной точке заготовки:

$a - T=20\text{ }^{\circ}\text{C}$ ;  $b - T=350\text{ }^{\circ}\text{C}$



**Fig. 5.** Change in the degree of deformation in a material point of the billet over time: **a** –  $T=20\text{ }^\circ\text{C}$ ; **b** –  $T=350\text{ }^\circ\text{C}$   
**Рис. 5.** Изменение во времени степени деформации в материальной точке заготовки: **a** –  $T=20\text{ }^\circ\text{C}$ ; **b** –  $T=350\text{ }^\circ\text{C}$



**Fig. 6.** Samples after one equal channel angular pressing (ECAP) pass:  
**a** –  $T=20\text{ }^\circ\text{C}$ ; **b** –  $T=400\text{ }^\circ\text{C}$  (arrow indicates the ECAP pass direction)  
**Рис. 6.** Образцы после одного прохода равноканального углового прессования (РКУП):  
**a** –  $T=20\text{ }^\circ\text{C}$ ; **b** –  $T=400\text{ }^\circ\text{C}$  (стрелкой указано направление прохода при РКУП)

## DISCUSSION

Functions (3) defining the plasticity of Mg–1%Zn–0.06%Ca magnesium alloy at temperatures of 20 and 350 °C, depending on the stress state index, established experimentally within the conducted studies correspond to the known pattern – the plasticity of magnesium alloys increases significantly with increasing temperature. The conducted studies have shown for the first time the possibility of successful application of the Cockcroft–Latham fracture model, taking into account the varying stress state [10], to the Mg–1%Zn–0.06%Ca alloy to determine the processing temperature. Until recently, this model was successfully applied to steels [14] and titanium

alloys [21]. Based on the results of computer simulation of the stress-strain state of the billet, and calculation of metal damage in the area with the most unfavorable stress state ( $\sigma_1 > 0$ ), it was decided to perform physical simulation of ECAP for the first pass at an initial temperature of the billet and tooling equal to 400 °C. This temperature was chosen with a conservative value, to ensure guaranteed nonfailure of the billet in the physical experiment. It was shown theoretically and experimentally that at the initial sample temperature of less than 250 °C, cracking occurs precisely in the area of the billet, where the  $c$  damage index has a maximum value according to the results of computer simulation. Earlier in the work [22],

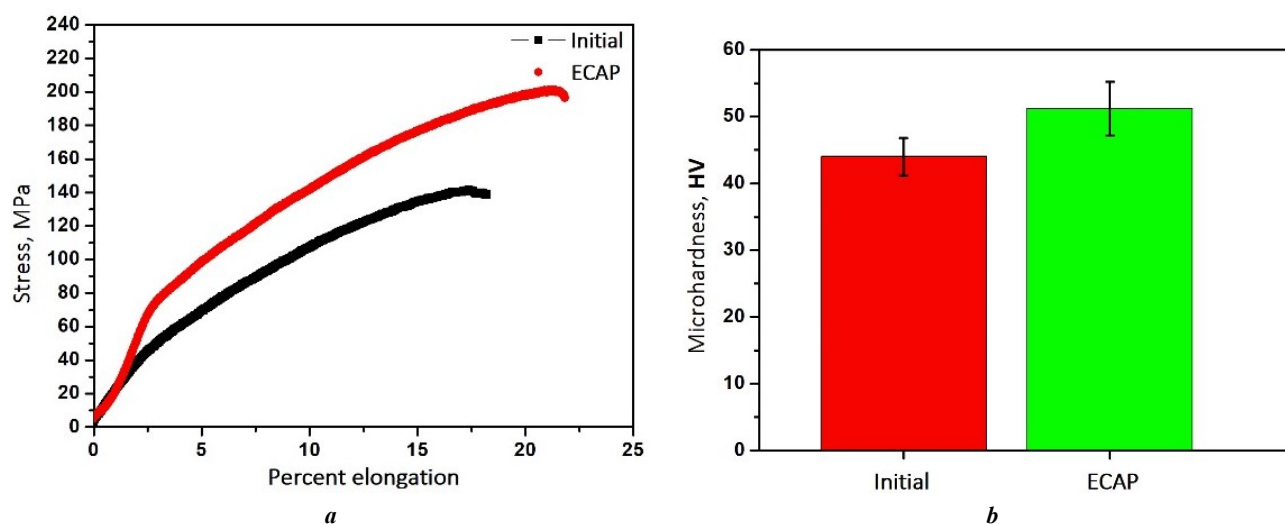


**Fig. 7.** Results of mechanical tests:

- a* – stress-strain curve of the Mg–1%Zn–0.06%Ca alloy before and after ECAP;  
*b* – comparison of the initial microhardness and microhardness obtained after ECAP

**Рис. 7.** Результаты механических испытаний:

- a* – диаграмма растяжения сплава Mg–1%Zn–0,06%Ca до и после РКУП;  
*b* – сравнение исходной и полученной после РКУП микротвердости

**Table 2.** Results of tensile tests of samples and microhardness measurements

**Таблица 2.** Результаты испытаний на растяжение образцов и измерения микротвердости

State	$T$ , °C	HV (average value)	$\sigma_{UTS}$ , MPa	$\sigma_{0.2}$ , MPa	$\delta$ , %
Initial state	20	44.0±2.8	144	42	18
After ECAP	20	51.2±3.4	210	68	23

similar behaviour of an alloy with a similar composition was noted for the specified processing temperature range.

Physical simulation of billets in 8 passes showed the successful use of a well-known approach, ECAP with a gradual decrease in the processing temperature [18], as applied to the Mg–1%Zn–0.06%Ca alloy. Samples that were not destroyed in the first pass at  $T=400$  °C were subjected to subsequent successful ECAP deformation in 7 more passes with a decrease in temperature from 400 to 250 °C.

The results of modelling the distribution of strain degree in the billet are in good agreement with the analytical estimate of the strain degree for 8 passes  $\varepsilon=5.04$  performed using the well-known formula [23]:

$$\varepsilon_i = \frac{N}{\sqrt{3}} \left[ 2 \operatorname{ctg} \left( \frac{\Phi}{2} + \frac{\Psi}{2} \right) + \Psi \cos \varepsilon c \left( \frac{\Phi}{2} + \frac{\Psi}{2} \right) \right], \quad (5)$$

where  $N$  is the number of passes;

$\Psi$  is the external angle;

$\Phi$  is the internal angle.

During the calculation, the external angle was taken to be 20°; the internal angle (the angle of intersection of

the channels corresponding to the equipment in Fig. 1) was 120°. The value of deformation of 0.63 for one ECAP pass calculated using formula (5) is in good agreement with the value obtained by modelling (Fig. 5).

As in [18], an increase in the mechanical properties of the magnesium alloy was found, but not as significant, which is due to the lower content of calcium in the composition: the tensile strength increased by 45 %, the hardness – by 16 % compared to the homogenised state. This is probably caused by the formation of a structure with a finer average grain size due to the increase in the strain degree to 5.

## CONCLUSIONS

1. The use of complex modelling of the process of severe plastic deformation of magnesium alloys, including computer and physical simulation on an experimental equipment, allows developing modes of billet deformation due to the alloy damage calculation using the Cockcroft–Latham model. Physical simulation of sample deformation confirmed the possibility of determining the thermomechanical mode of ECAP of a magnesium alloy of the Mg–Zn–Ca system, which ensures

deformation of samples without destruction, by computer simulation. The results of physical modelling are in good agreement with the values of damage calculated during computer simulation: room temperature  $\omega=1.19$  ( $\omega \geq 1$ , failure condition) corresponded to sample failure during severe plastic deformation;  $T=350$  °C and  $\omega=0.9$  ( $\omega < 1$ , nonfailure condition) corresponded to nonfailure of the sample. This demonstrates the reliability of the processing mode obtained by complex modelling and the validity of its application to bulk billets.

2. Severe plastic deformation is an effective method for improving mechanical properties: after 8 ECAP passes, the alloy strength values increased from 144 to 210 MPa, which is 45 % higher compared to the homogenised state of the untreated sample, the microhardness value increased as well from  $44 \pm 2.8$  to  $51.2 \pm 3.4$  HV.

## REFERENCES

- Sun Yu, Zhang Baoping, Wang Yin, Geng Lin, Jiao Xiaohu. Preparation and characterization of a new biomedical Mg-Zn-Ca alloy. *Materials and Design*, 2012, vol. 34, pp 58–64. DOI: [10.1016/j.matdes.2011.07.058](https://doi.org/10.1016/j.matdes.2011.07.058).
- Vinogradov A., Merson E., Myagkikh P., Linderov M., Brilevsky A., Merson D. Attaining High Functional Performance in Biodegradable Mg-Alloys: An Overview of Challenges and Prospects for the Mg-Zn-Ca System. *Materials*, 2023, vol. 16, no. 3, article number 1324. DOI: [10.3390/ma16031324](https://doi.org/10.3390/ma16031324).
- Valiev R.Z., Zhilyaev A.P., Lengdon T.Dzh. *Obemnyye nanostrukturnyye materialy: fundamentalnyye osnovy i primeneniya* [Bulk nanostructural materials: fundamental principle and application]. Sankt Petersburg, Eko-Vektor Publ., 2017. 479 p.
- Martynenko N.S., Anisimova N.Y., Rybalchenko O.V. et al. Rationale for Processing of a Mg-Zn-Ca Alloy by Equal-Channel Angular Pressing for Use in Biodegradable Implants for Osteoreconstruction. *Crystals*, 2021, vol. 11, article number 1381. DOI: [10.3390/cryst11111381](https://doi.org/10.3390/cryst11111381).
- Medeiros M.P., Lopes D.R., Kawasaki M., Langdon T.G., Figueiredo R.B. An Overview on the Effect of Severe Plastic Deformation on the Performance of Magnesium for Biomedical Applications. *Materials*, 2023, vol. 16, no. 6, article number 2401. DOI: [10.3390/ma16062401](https://doi.org/10.3390/ma16062401).
- Rezaei-Baravati A., Kasiri-Asgarani M., Bakhsheshi-Rad H.R., Omidi M., Karamian E. Microstructure, Biodegradation, and Mechanical Properties of Biodegradable Mg-Based Alloy Containing Calcium for Biomedical Applications. *Physical Mesomechanics*, 2023, vol. 26, no. 2, pp. 176–195. DOI: [10.1134/S1029959923020078](https://doi.org/10.1134/S1029959923020078).
- Alper Incesu, Ali Gungor. Mechanical properties and biodegradability of Mg-Zn-Ca alloys: homogenization heat treatment and hot rolling. *Journal of materials science. Materials in medicine*, 2020, vol. 31, no. 12, article number 123. DOI: [10.1007/s10856-020-06468-5](https://doi.org/10.1007/s10856-020-06468-5).
- Roche V., Koga G.Y., Matias T.B., Kiminami C.S., Bolfarini C., Botta W.J., Nogueira R.P., Jorge Junior A.M. Degradation of Biodegradable Implants: The Influence of Microstructure and Composition of Mg-Zn-Ca Alloys. *Journal of Alloys and Compounds*, 2019, vol. 774, pp. 168–181. DOI: [10.1016/j.jallcom.2018.09.346](https://doi.org/10.1016/j.jallcom.2018.09.346).
- Kolmogorov V.L. Numerical simulation of large plastic deformations and failure of metals. *Kuznechno-shtampovochnoye proizvodstvo*, 2003, no. 2, pp. 4–16.
- Botkin A.V., Valiev R.Z., Stepin P.S., Baymukhamev A.Kh. Estimation of metal damage during cold plastic deformation using the Cockcroft–Latham failure model. *Deformatsiya i razrusheniye materialov*, 2011, no. 7, pp. 17–22. EDN: [NXAHSN](https://www.edn.net/NXAHSN).
- Kwak Eun Jeong, Bok Cheon Hee, Seo Min Hong, Kim Taek-Soo, Kim Hyoung Seop. Processing and mechanical properties of fine-grained magnesium by equal channel angular pressing. *Materials Transactions*, 2008, vol. 49, no. 5, pp. 1006–1010. DOI: [10.2320/matertrans.MC200725](https://doi.org/10.2320/matertrans.MC200725).
- Christiansen P., Nielsen C.V., Martins P.A.F., Bay N. Predicting the onset of cracks in bulk metal forming by ductile damage criteria. *Procedia Engineering*, 2017, vol. 207, pp. 2048–2053. DOI: [10.1016/j.proeng.2017.10.1106](https://doi.org/10.1016/j.proeng.2017.10.1106).
- Vlasov A.V. On the application of the Cockcroft–Latham criterion to predict fracture in cold forging. *Izvestiya Tul'skogo gosudarstvennogo universiteta. Tekhnicheskie nauki*, 2017, no. 11-1, pp. 46–58. EDN: [ZVLXNV](https://www.edn.net/ZVLXNV).
- Matveev M.A. Numerical estimation of the probability of metal failure under hot plastic deformation by means of the Cockcroft – Latham criterion. *Nauchno-tekhnicheskie vedomosti SPbPU. Estestvennye i inzhenernye nauki*, 2017, vol. 23, no. 2, pp. 109–126. DOI: [10.18721/JEST.230211](https://doi.org/10.18721/JEST.230211).
- Shtremel M.A. *Razrusheniye. Razrusheniye materialov* [Destruction. Destruction of materials]. Moscow, MISIS Publ., 2014. Kn. 1, 670 p.
- Chen Xuewen, Yang Zhen, Zhang Bo, Sun Jiawei, Su Zhiyi, Mao Yiran. An Inverse Optimization Method for the Parameter Determination of the High-Temperature Damage Model and High-Temperature Damage Graph of Ti6Al4V Alloy. *Materials*, 2023, vol. 16, article number 4770. DOI: [10.3390/ma16134770](https://doi.org/10.3390/ma16134770).
- Khudododova G.D., Kulyasova O.B., Nafikov R.K., Islamgaliev R.K. The structure and mechanical properties of biomedical magnesium alloy Mg–1%Zn–0.2%Ca. *Frontier Materials & Technologies*, 2022, no. 2, pp. 105–112. DOI: [10.18323/2782-4039-2022-2-105-112](https://doi.org/10.18323/2782-4039-2022-2-105-112).
- Kulyasova O.B., Islamgaliev R.K. The influence of the structural changes in the Mg-1%Zn-0,2%Ca alloy, produced by ECAP on its mechanical properties. *Vestnik Ufimskogo gosudarstvennogo aviatsionnogo tekhnicheskogo universiteta*, 2018, vol. 22, no. 3, pp. 24–29. EDN: [YAAWLZ](https://www.edn.net/YAAWLZ).
- Cockcroft M.G., Latham D.J. Ductility and Workability of metals. *Journal of the Institute of Metals*, 1968, vol. 96, pp. 33–39.
- Botkin A.V., Valiev R.Z., Kublikova A.A., Dubinina S.V. Determining the shear plasticity of metals on the basis of torsion-tension tests. *Steel in Translation*, 2013, vol. 43, no. 6, pp. 360–364. DOI: [10.3103/S096709121306003X](https://doi.org/10.3103/S096709121306003X).
- Gao Lin, Zhao Jiang, Quan Guo-zheng, Xiong Wei, An Chao. Study on the Evolution of Damage Degradation



- tion at Different Temperatures and Strain Rates for Ti-6Al-4V Alloy. *High Temperature Materials and Processes*, 2018, vol. 38, pp. 332–341. DOI: [10.1515/htmp-2018-0091](https://doi.org/10.1515/htmp-2018-0091).
22. Kozulyan A.A., Skripnyak V.A., Krasnoveikin V.A., Skripnyak V.V., Karavatskii A.K. An investigation of physico-mechanical properties of ultrafine-grained magnesium alloys subjected to severe plastic deformation. *Russian Physics Journal*, 2015, vol. 57, no. 9, pp. 1261–1267. DOI: [10.1007/s11182-015-0372-5](https://doi.org/10.1007/s11182-015-0372-5).
  23. Iwahashi Y., Wang J., Horita Z., Nemoto M., Langdon T.G. Principle of equal-channel angular pressing for the processing of ultra-fine-grained materials. *Scripta Materialia*, 1996, vol. 35, no. 2, pp. 143–146. DOI: [10.1016/1359-6462\(96\)00107-8](https://doi.org/10.1016/1359-6462(96)00107-8).
- ### СПИСОК ЛИТЕРАТУРЫ
1. Sun Yu, Zhang Baoping, Wang Yin, Geng Lin, Jiao Xiaohu. Preparation and characterization of a new biomedical Mg-Zn-Ca alloy // *Materials and Design*. 2012. Vol. 34. P. 58–64. DOI: [10.1016/j.matdes.2011.07.058](https://doi.org/10.1016/j.matdes.2011.07.058).
  2. Vinogradov A., Merson E., Myagkikh P., Linderov M., Brilevsky A., Merson D. Attaining High Functional Performance in Biodegradable Mg-Alloys: An Overview of Challenges and Prospects for the Mg-Zn-Ca System // *Materials*. 2023. Vol. 16. № 3. Article number 1324. DOI: [10.3390/ma16031324](https://doi.org/10.3390/ma16031324).
  3. Валиев Р.З., Жилиев А.П., Лэнгдон Т.Дж. Объемные наноструктурные материалы: фундаментальные основы и применения. СПб.: Эко-Вектор, 2017. 479 с.
  4. Martynenko N.S., Anisimova N.Y., Rybalchenko O.V. et al. Rationale for Processing of a Mg-Zn-Ca Alloy by Equal-Channel Angular Pressing for Use in Biodegradable Implants for Osteoreconstruction // *Crystals*. 2021. Vol. 11. Article number 1381. DOI: [10.3390/cryst11111381](https://doi.org/10.3390/cryst11111381).
  5. Medeiros M.P., Lopes D.R., Kawasaki M., Langdon T.G., Figueiredo R.B. An Overview on the Effect of Severe Plastic Deformation on the Performance of Magnesium for Biomedical Applications // *Materials*. 2023. Vol. 16. № 6. Article number 2401. DOI: [10.3390/ma16062401](https://doi.org/10.3390/ma16062401).
  6. Rezaei-Baravati A., Kasiri-Asgarani M., Bakhsheshi-Rad H.R., Omidi M., Karamian E. Microstructure, Biodegradation, and Mechanical Properties of Biodegradable Mg-Based Alloy Containing Calcium for Biomedical Applications // *Physical Mesomechanics*. 2023. Vol. 26. № 2. P. 176–195. DOI: [10.1134/S1029959923020078](https://doi.org/10.1134/S1029959923020078).
  7. Alper Incesu, Ali Gungor. Mechanical properties and biodegradability of Mg-Zn-Ca alloys: homogenization heat treatment and hot rolling // *Journal of materials science. Materials in medicine*. 2020. Vol. 31. № 12. Article number 123. DOI: [10.1007/s10856-020-06468-5](https://doi.org/10.1007/s10856-020-06468-5).
  8. Roche V., Koga G.Y., Matias T.B., Kiminami C.S., Bolfarini C., Botta W.J., Nogueira R.P., Jorge Junior A.M. Degradation of Biodegradable Implants: The Influence of Microstructure and Composition of Mg-Zn-Ca Alloys // *Journal of Alloys and Compounds*. 2019. Vol. 774. P. 168–181. DOI: [10.1016/j.jallcom.2018.09.346](https://doi.org/10.1016/j.jallcom.2018.09.346).
  9. Колмогоров В.Л. Численное моделирование больших пластических деформаций и разрушения металлов // *Кузнечно-штамповочное производство*. 2003. № 2. С. 4–16.
  10. Боткин А.В., Валиев Р.З., Степин П.С., Баймухаметов А.Х. Оценка поврежденности металла при холодной пластической деформации с использованием модели разрушения Кокрофт – Латам // *Деформация и разрушение материалов*. 2011. № 7. С. 17–22. EDN: [NXAHSN](https://www.edn.ru/NXAHSN).
  11. Kwak Eun Jeong, Bok Cheon Hee, Seo Min Hong, Kim Taek-Soo, Kim Hyoung Seop. Processing and mechanical properties of fine-grained magnesium by equal channel angular pressing // *Materials Transactions*. 2008. Vol. 49. № 5. P. 1006–1010. DOI: [10.2320/matertrans.MC200725](https://doi.org/10.2320/matertrans.MC200725).
  12. Christiansen P., Nielsen C.V., Martins P.A.F., Bay N. Predicting the onset of cracks in bulk metal forming by ductile damage criteria // *Procedia Engineering*. 2017. Vol. 207. P. 2048–2053. DOI: [10.1016/j.proeng.2017.10.1106](https://doi.org/10.1016/j.proeng.2017.10.1106).
  13. Власов А.В. О применении критерия Кокрофта – Лэтэма для прогнозирования разрушения при холодной объемной штамповке // *Известия Тульского государственного университета. Технические науки*. 2017. № 11-1. С. 46–58. EDN: [ZVLXNV](https://www.edn.ru/ZVLXNV).
  14. Матвеев М.А. Оценка вероятности разрушения металла при горячей пластической деформации с помощью критерия Кокрофта – Латама // *Научно-технические ведомости СПбПУ. Естественные и инженерные науки*. 2017. Т. 23. № 2. С. 109–126. DOI: [10.18721/JEST.230211](https://doi.org/10.18721/JEST.230211).
  15. Штремель М.А. Разрушение. В 2-х кн. Кн. 1: Разрушение материалов. М.: МИСИС, 2014. 670 с.
  16. Chen Xuewen, Yang Zhen, Zhang Bo, Sun Jiawei, Su Zhiyi, Mao Yiran. An Inverse Optimization Method for the Parameter Determination of the High-Temperature Damage Model and High-Temperature Damage Graph of Ti6Al4V Alloy // *Materials*. 2023. Vol. 16. Article number 4770. DOI: [10.3390/ma16134770](https://doi.org/10.3390/ma16134770).
  17. Худододова Г.Д., Кулясова О.Б., Нафиков Р.К., Исламгалиев Р.К. Структура и механические свойства биомедицинского магниевое сплава Mg-1%Zn-0,2%Ca // *Frontier Materials & Technologies*. 2022. № 2. С. 105–112. DOI: [10.18323/2782-4039-2022-2-105-112](https://doi.org/10.18323/2782-4039-2022-2-105-112).
  18. Кулясова О.Б., Исламгалиев Р.К. Влияние структурных изменений на механические свойства сплава Mg-1%Zn-0,2%Ca, полученного методом равноканального углового прессования // *Вестник Уфимского государственного авиационного технического университета*. 2018. Т. 22. № 3. С. 24–29. EDN: [YAAWLZ](https://www.edn.ru/YAAWLZ).
  19. Cockcroft M.G., Latham D.J. Ductility and Workability of metals // *Journal of the Institute of Metals*. 1968. Vol. 96. P. 33–39.
  20. Боткин А.В., Валиев Р.З., Кубликова А.А., Дубинина С.В. Исследование пластичности металла при сдвиге на основе результатов испытаний образцов кручением, совместным с растяжением (сжатием) // *Известия высших учебных заведений. Черная металлургия*. 2013. № 6. С. 60–65. DOI: [10.17073/0368-0797-2013-6-60-65](https://doi.org/10.17073/0368-0797-2013-6-60-65).
  21. Gao Lin, Zhao Jiang, Quan Guo-zheng, Xiong Wei, An Chao. Study on the Evolution of Damage Degradation

- tion at Different Temperatures and Strain Rates for Ti-6Al-4V Alloy // High Temperature Materials and Processes. 2018. Vol. 38. P. 332–341. DOI: [10.1515/htmp-2018-0091](https://doi.org/10.1515/htmp-2018-0091).
22. Козулин А.А., Скрипняк В.А., Красновейкин В.А., Скрипняк В.В., Каравацкий А.К. Исследование физико-механических свойств ультрамелкозернистых магниевых сплавов после интенсивной пластической деформации // Известия высших учебных заведений. Физика. 2014. Т. 57. № 9. С. 98–104. EDN: [SXZFZX](https://www.edn.ru/SXZFZX).
23. Iwahashi Y., Wang J., Horita Z., Nemoto M., Langdon T.G. Principle of equal-channel angular pressing for the processing of ultra-fine-grained materials // Scripta Materialia. 1996. Vol. 35. № 2. P. 143–146. DOI: [10.1016/1359-6462\(96\)00107-8](https://doi.org/10.1016/1359-6462(96)00107-8).

## Компьютерное прогнозирование разрушения цилиндрической заготовки из магниевого сплава в процессе равноканального углового прессования

**Волкова Елена Павловна**<sup>1</sup>, младший научный сотрудник

Научно-исследовательского института физики перспективных материалов

**Худододова Ганджина Дастамбуевна**<sup>2</sup>, младший научный сотрудник

Научно-исследовательского института физики перспективных материалов

**Боткин Александр Васильевич**<sup>3</sup>, доктор технических наук,

профессор кафедры материаловедения и физики металлов

**Валиев Руслан Зуфарович**<sup>\*4</sup>, доктор физико-математических наук, профессор,

директор Научно-исследовательского института физики перспективных материалов

Уфимский университет науки и технологий, Уфа (Россия)

\*E-mail: [ruslan.valiev@ugatu.su](mailto:ruslan.valiev@ugatu.su)

<sup>1</sup>ORCID: <https://orcid.org/0009-0004-7183-4077>

<sup>2</sup>ORCID: <https://orcid.org/0000-0002-1273-8518>

<sup>3</sup>ORCID: <https://orcid.org/0000-0001-9522-280X>

<sup>4</sup>ORCID: <https://orcid.org/0000-0003-4340-4067>

Поступила в редакцию 03.05.2024

Пересмотрена 18.09.2024

Принята к публикации 21.10.2024

**Аннотация:** Основной сложностью в использовании магниевых сплавов, применяемых в медицине в качестве биоразлагаемых материалов, является труднодеформируемость, что, в свою очередь, приводит к частым разрушениям образцов во время интенсивной пластической деформации. В работе показано, что температурный режим равноканального углового прессования (РКУП) магниевого сплава системы Mg–Zn–Ca, обеспечивающий деформирование образцов без разрушения, возможно определять по результатам конечно-элементного компьютерного моделирования напряженно-деформированного состояния заготовки, расчета поврежденности сплава с использованием модели Кокрофта – Лэтэма и прогнозирования области разрушения образца. Моделирование показало, что поверхностная область заготовки, примыкающая при РКУП к внутреннему углу матрицы, является областью возможного разрушения магниевого сплава. Значение поврежденности сплава при РКУП в этой области при  $T=350$  °C меньше 1, что соответствует неразрушению металла. Для верификации результатов компьютерного моделирования выполнено физическое моделирование РКУП, получены заготовки без признаков разрушения. Произведено исследование механических свойств магниевого сплава Mg–1%Zn–0,06%Ca до и после обработки РКУП по выбранному режиму: предел прочности повысился на 45 %, твердость увеличилась на 16 %, при этом пластичность повысилась на 5 %.

**Ключевые слова:** магниевые сплавы; напряженно-деформированное состояние; конечно-элементное компьютерное моделирование; поврежденность сплава; равноканальное угловое прессование; микротвердость; предел прочности.

**Благодарности:** Работа выполнена при поддержке РФФИ, проект № 24-43-20015 (<https://rscf.ru/project/24-43-20015/>). Экспериментальная часть работы выполнена с использованием оборудования ЦКП «Нанотех» ФГБОУ ВО «УУНиТ».

**Для цитирования:** Волкова Е.П., Худододова Г.Д., Боткин А.В., Валиев Р.З. Компьютерное прогнозирование разрушения цилиндрической заготовки из магниевого сплава в процессе равноканального углового прессования // Frontier Materials & Technologies. 2024. № 4. С. 19–28. DOI: [10.18323/2782-4039-2024-4-70-2](https://doi.org/10.18323/2782-4039-2024-4-70-2).